Terrestrial cooling in Northern Europe during the Eocene–Oligocene transition

Michael T. Hren[a,b,1], Nathan D. Sheldon[c], Stephen T. Grimes[d], Margaret E. Collinson[e], Jerry J. Hooker[f], Melanie Bugler[d], and Kyger C. Lohmann[c]

[a]Department of Chemistry and [b]Center for Integrative Geoscience, University of Connecticut, Storrs, CT 06269; [c]Department of Earth and Environmental Sciences, University of Michigan, Ann Arbor, MI 48109; [d]School of Geography, Earth and Environmental Sciences, University of Plymouth, Plymouth, Devon PL4 8AA, United Kingdom; [e]Department of Earth Sciences, Royal Holloway University of London, Egham, Surrey TW20 0EX, United Kingdom; and [f]Department of Palaeontology, Natural History Museum, London SW7 5BD, United Kingdom

Geochemical and modeling studies suggest that the transition from the "greenhouse" state of the Late Eocene to the "icehouse" conditions of the Oligocene 34–33.5 Ma was triggered by a reduction of atmospheric pCO$_2$ that enabled the rapid buildup of a permanent ice sheet on the Antarctic continent. Marine records show that the drop in pCO$_2$ during this interval was accompanied by a significant decline in high-latitude sea surface and deep ocean temperature and enhanced seasonality in middle and high latitudes. However, terrestrial records of this climate transition show heterogeneous responses to changing pCO$_2$ and ocean temperatures, with some records showing a significant time lag in the temperature response to declining pCO$_2$. We measured the Δ_{47} of aragonite shells of the freshwater gastropod *Viviparus lentus* from the Solent Group, Hampshire Basin, United Kingdom, to reconstruct terrestrial temperature and hydrologic change in the North Atlantic region during the Eocene–Oligocene transition. Our data show a decrease in growing-season surface water temperatures (~10 °C) during the Eocene–Oligocene transition, corresponding to an average decrease in mean annual air temperature of ~4–6 °C from the Late Eocene to Early Oligocene. The magnitude of cooling is similar to observed decreases in North Atlantic sea surface temperature over this interval and occurs during major glacial expansion. This suggests a close linkage between atmospheric carbon dioxide concentrations, Northern Hemisphere temperature, and expansion of the Antarctic ice sheets.

clumped isotopes | paleoclimate

The Eocene–Oligocene transition 34–33.5 Ma represents one of the most dramatic climatic changes of the past 65 My (1–3). Studies suggest that by 34 Ma, pCO$_2$ reached a critical threshold where favorable orbital parameters and ocean circulation patterns allowed the rapid buildup of Antarctic ice, triggering widespread reduction in atmospheric pCO$_2$ and decreases in sea surface and deep ocean temperature (4–8). This event is marked by a +1.5‰ shift in the oxygen isotope ratios of carbonate from deep-sea benthic foraminifera, which reflects both the glaciation of Antarctica and rapid cooling of the surface and deep ocean (1, 3).

Marine sediments provide high-resolution records of surface and deep ocean temperature responses to the Late Eocene decreases in pCO$_2$ and Antarctic glaciation (7, 8). These show that cooling was amplified in high-latitude regions, with a decrease in sea surface temperature of >5 °C from the Late Eocene to Early Oligocene (7). Tropical sea surface temperature (SST) and deep ocean records show mixed responses to global cooling across the Eocene–Oligocene transition (EOT), with some indicating only modest declines in temperature in the tropics (8) and others showing a 3–4 °C decrease in SST during the first stage of the cooling event (EOT-1) (9). One recent multiproxy study suggests that cooling during the EOT was specifically linked to increased seasonality, with the majority of cooling occurring during the cool-season months (9).

There are relatively few terrestrial records of the EOT from the mid- to high latitudes, and terrestrial paleoclimate data show heterogeneous climate responses. Some records show no major climatic changes during the EOT glaciation (6, 10) and others show cooling of 8 °C (11), increased seasonality (9, 12), and aridification (13). This discrepancy confounds efforts to determine the timescale and sensitivity of terrestrial climate response to changing atmospheric pCO$_2$ or ocean circulation. We measure the δ^{18}O and Δ_{47} of CO$_2$ derived from carbonate shells of the freshwater gastropod *Viviparus lentus* from the Hampshire Basin, United Kingdom. (Fig. S1). Our results provide unique constraints on Northern Hemisphere terrestrial paleoclimate change during the EOT and indicate cooling of ~4–6 °C in mean annual air temperatures (MAAT) in northern Europe in response to atmospheric CO$_2$ reductions and Antarctic glaciation.

Results and Discussion

Solent Group Stratigraphy and Paleoclimate. Terrestrial records of Late Eocene European climate are rare; however, continental sediments of the Solent Group in the Hampshire Basin (Isle of Wight, United Kingdom) provide an age-calibrated (*SI Methods*) terrestrial EOT record from the mid-North Atlantic region. Sediments of the Solent Group were deposited in a coastal plain setting at ~45–50°N from the Late Eocene through the Early Oligocene and have never been deeply buried, and nearly all remain unlithified (14). Throughout the sequence, freshwater lacustrine and alluvial sediments are punctuated by a few brief marine incursions that help provide age control (15).

Fossils from the Hampshire Basin indicate a warm Late Eocene climate with abundant marsh vegetation, palms, fruit-eating mammals, and crocodilians (14–17). δ^{18}O of carbonate from freshwater gastropods, fossil rodent teeth, and charophytes within Solent Group sediments has been interpreted to show peak Late Eocene freshwater summer temperatures of >30 °C, with only minor reduction in growing season temperature across the EOT (10, 15, 18). However, δ^{18}O-derived temperatures contrast with North Atlantic SST and paleofloral data (6, 7), which record significant temperature decreases across the EOT. These also contradict δ^{18}O data from North American fossils that show an ~8 °C cooling during this same time (11). One complication with conventional δ^{18}O temperature interpretations is that they rely on estimates of the δ^{18}O$_{water}$ at the time of formation. Changes in the isotopic composition of precipitation or ambient water (e.g., due to evaporation) can introduce uncertainty in reconstructions of

paleotemperature in the Late Eocene to Early Oligocene of the Hampshire Basin (10).

Clumped Isotope Paleothermometry. The "clumped isotope thermometer" is a temperature proxy based on a measure of the temperature-dependent abundance of doubly substituted ^{13}C and ^{18}O isotopes that are bound to each other within the carbonate lattice (19). The Δ_{47} of carbonate minerals [a measure of the abundance anomaly of ^{13}C-^{18}O bonds in carbonate-derived CO_2 and defined as $\Delta_{47} = (R^{47}_{actual}/R^{47}_{stochastic} - 1) \times 1,000$] provides a measure of formation temperature, $\delta^{13}C$, and $\delta^{18}O$ of carbonate and allows direct calculation of $\delta^{18}O$ of parent water (20).

Δ_{47} Measurements and Data Reduction. We collected shells of the freshwater prosobranch gastropod *V. lentus* from five localities within the Solent Group of the Hampshire Basin, Isle of Wight, for $\delta^{18}O$ and Δ_{47} temperature measurement. Samples were collected from 10 intervals that span nearly 3 My of the Late Eocene to Early Oligocene (Table S1). Sediments were dried, disaggregated, and sieved to separate shell materials. Shells were embedded in epoxy for thin-section analyses (Figs. S2 and S3). For high-resolution $\delta^{18}O$, complete shells were broken into consecutive pieces, and each was supported internally by epoxy and microsampled. Shell fragments for Δ_{47} measurements were crushed to a size fraction of <400 μm and stored in a dry chamber before analysis. Splits of this fraction were crushed to <200 μm, using an agate mortar and pestle immediately before Δ_{47} analysis. Each sample line (Table S1 and Dataset S1) represents a measurement of a split of the <400-μm fraction and two to four splits are used to determine the sample level mean for Δ_{47}. Variability between splits reflects any heterogeneity preserved in the <400-μm fraction.

$\delta^{13}C$, $\delta^{18}O$, and Δ_{47} of purified CO_2 were measured on a Thermo Finnigan MAT 253 mass spectrometer configured to measure masses 44–49 with sample and reference gas capillaries balanced at a 16-V signal (*Methods*). Sample gas was measured against a reference of known isotopic composition for a total of 8–10 replicates of 10 cycles. Δ_{47} values were determined using established methods (19) and normalized through analysis of CO_2 gas with a range of isotopic compositions that was heated for 2 h at 1,000 °C to achieve the "near"-stochastic distribution of isotopologues. Δ_{48} values provide a check for contaminants with interfering masses that could impact Δ_{47}, and gas with high measured Δ_{48} values was excluded from our data.

To relate Δ_{47} measurements to temperature using the empirically determined Δ_{47}-temperature relationship of Ghosh et al. (20), it is critical to correct for scale compression of individual mass spectrometers (21). Our measurements predate establishment of the "Absolute Reference Frame" (ARF) and normalization procedures outlined therein (22). As a result, we normalized Δ_{47} data to the ARF (Figs. S4 and S5), using measured Δ_{47} of CO_2 of varied isotopic composition and equilibrated with water at 25 °C, a Carrara marble sample that has been run numerous times and in multiple laboratories, and gases of varied composition heated to 1,000 °C (*SI Methods* and Table S2).

Gastropod Δ_{47} Temperatures. Calibration of the clumped isotope thermometer derives from a variety of biotic and abiotic carbonates from a range of growth temperatures (20). Studies show that molluscs precipitate carbonate in isotopic equilibrium (23), and mollusc Δ_{47} data fall on the empirical Δ_{47}-temperature calibration curve of Ghosh et al. (20). Recent study of Δ_{47} of two species of aquatic gastropods in freshwater Pliocene sediments shows no temperature bias related to "vital effects" during gastropod growth and demonstrates that gastropod carbonate precipitates in equilibrium with ambient waters (24). Our examination of a modern unionid mollusc from the Huron River in Michigan produces a Δ_{47} temperature of ~19 °C, which compares favorably to mean May to September growing season temperatures that average 19.6 °C

(PRISM Climate Group). These data show that Δ_{47} temperatures for aquatic gastropods reliably match conventional oxygen isotope paleothermometry estimates when water $\delta^{18}O$ is well constrained, unlike terrestrial gastropod Δ_{47} temperatures (25). However, aquatic gastropod Δ_{47} data are biased by seasonal temperature variation during the period of shell growth.

Multiple lines of evidence indicate that our Δ_{47} data record primary values. First, fossil shells are preserved in clay-rich sediments, which potentially reduced fluid-flow that could have altered the primary shell structure during burial. Second, Solent Group sediments have not been deeply buried, heated, or extensively altered, and most sediments remain unlithified (14–16, 26). Although low-temperature diagenetic alteration of aragonite to secondary calcite is commonly observed in the rock record (27), all samples were analyzed by X-ray diffraction and produced patterns consistent with aragonite (28). Third, thin-section analyses of individual shells showed an outer layer with vertical crystals in all shells. The prismatic, alternating vertical crystals and clear growth cessation marks are consistent with modern *Viviparus* species (Fig. 1 and Figs. S2 and S3), indicating preservation of primary structure. Finally, we conducted high-resolution microsampling of five pristine shells to examine the variability in $\delta^{18}O$ of individual shells across the EOT (Fig. 2). These all preserve fine-scale $\delta^{18}O$ variations that reflect changes in water temperature and composition during the period of shell growth. These data also show a decrease in $\delta^{18}O$ values during the EOT, consistent with changes in local environmental conditions. Preservation of variability on the millimeter scale within the aragonite shell matrix suggests original Δ_{47} values have also not been altered.

Δ_{47} Temperature Data and Paleoclimate. Aquatic gastropods are incapable of regulating body temperature, so shell carbonate is precipitated in thermal equilibrium with ambient water (29). As a result, $\Delta_{47\ shell}$ of ancient gastropods records seasonal growth
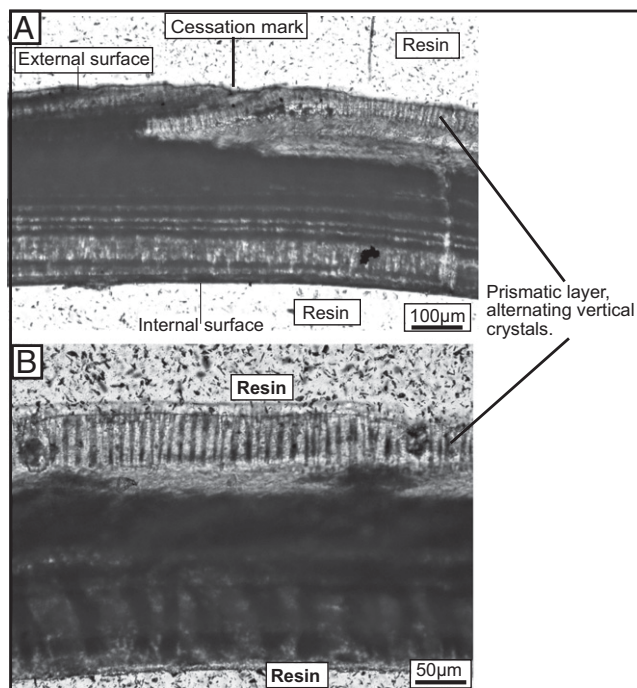
Fig. 1. (*A*) Thin section of a Late Eocene *V. lentus* in plane light. The shell structure contains a prismatic layer with alternating vertical crystals similar to those of modern shells and clear cessation marks that show the interruption of shell growth due to food or temperature reductions. (*B*) Detail of prismatic layer.
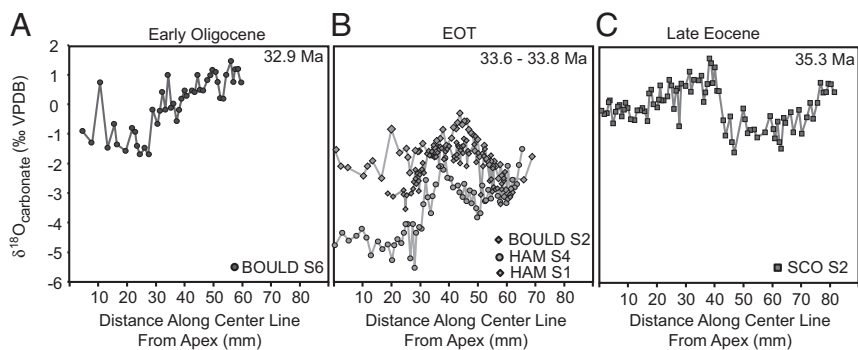
Fig. 2. (A–C) Subannual $\delta^{18}O$ record of (A) Early Oligocene, (B) Eocene–Oligocene, and (C) Late Eocene gastropods. Sample ages are shown in upper right corner. Isotopic variability shows preservation of primary $\delta^{18}O$ variations due to temperature or water $\delta^{18}O$ changes. Shells from the EOT are marked by a shift to low $\delta^{18}O$ values, the lowest (sample HAM S4) of which occurs at 33.7 Ma and corresponds to the interval of the coldest Δ_{47} temperatures during the EOT.

temperature. This can be related to MAAT, providing a clear picture of ΔT (°C) across the EOT. Our samples span the EOT reduction in atmospheric CO_2 and Oligocene oxygen isotope event 1 (Oi-1) (Oi-1 onset between samples BOULD S1 and BOULD S5), although no fossil carbonates are available from the peak of the Oi-1 glacial event due to sea-level fall that interrupted deposition (15).

Because of the large sample size required for Δ_{47} measurements (5–10 mg), we homogenized individual gastropod shell fragments to <400 μm and powdered individual sample splits immediately to <200 μm before analysis. Two to four splits of the coarser fraction were measured for Δ_{47} to determine "bulk" growth temperature for each sample unit. This approach has the benefit of enabling precise measurement of bulk growth temperature; however, it integrates any seasonal temperature variability as shown by the high-resolution $\delta^{18}O$ data (Fig. 2). This produces a single measure of growing season temperature that is weighted proportionally to periods of higher metabolic and carbonate accumulation rates. Our data show slightly greater bulk isotopic variability between sample splits relative to standard materials, suggesting some heterogeneity at the <400-μm scale.

Sample mean Δ_{47} values range from 0.671 to 0.735 relative to the ARF (22) (Fig. 3A and Table S1). There is debate over temperature calibrations for some types of carbonates (20, 22, 30) and differences between calibrations produce large discrepancies for low temperatures (<15 °C). We use the calibration of Ghosh et al. (20) recalculated to the ARF (22) and assume temperatures reflect the time-integrated water T °C over the period of shell growth. Using this calibration, Δ_{47} values correspond to water temperatures of 34–20 °C. Before 34 Ma, growing season water temperatures range from 28 to 34 °C, with peak temperatures occurring before the EOT (Fig. 3B). Measured values are similar to June to September mean surface water temperatures from subtropical areas such as the Florida Everglades (*SI Methods*), an area with a broadly similar climate to that of the Late Eocene Hampshire Basin (16). Growing season temperatures oscillate during initial phases of ice buildup on Antarctica (within EOT, Fig. 3B). Following the major pCO_2 reduction, growing season water temperatures decline significantly from pre-EOT values, ranging from 20 to 24 °C (Fig. 3 A and B).

$\delta^{18}O$ of Eocene–Oligocene Waters. The $\delta^{18}O_{gastropod}$ depends on the $\delta^{18}O_{water}$ and temperature during the formation of shell carbonate. Δ_{47} temperature data allow calculation of $\delta^{18}O$ water across the EOT, using a temperature-dependent aragonite–water fractionation equation (31):

$$1,000 LN\alpha = \left(2.559 \times 10^6\right)/T^2 + 0.715.$$

$\delta^{18}O_{water}$ is highly evaporative before the EOT, coinciding with a period of high pCO_2, high growth temperatures (~34 °C), and a water $\delta^{18}O$ of ~ +3‰. Following the decline in pCO_2 (5) and

associated changes in marine $\delta^{18}O$ data (8), Hampshire Basin $\delta^{18}O_{water}$ returns to pre-EOT compositions despite a shift of the ocean $\delta^{18}O$ due to the buildup of Antarctic ice (2). Reconstructed water $\delta^{18}O$ values are more positive than those of seawater, reflecting highly evaporative conditions during the EOT (Table S1). Calculated water $\delta^{18}O$ from Hampshire Basin gastropods shows significant variability before and during the EOT. This variability is similar to that observed in contemporaneous sediments in the Ebro Basin, Spain, which show significant changes to the hydrologic cycle in the Late Eocene and Early Oligocene (32).
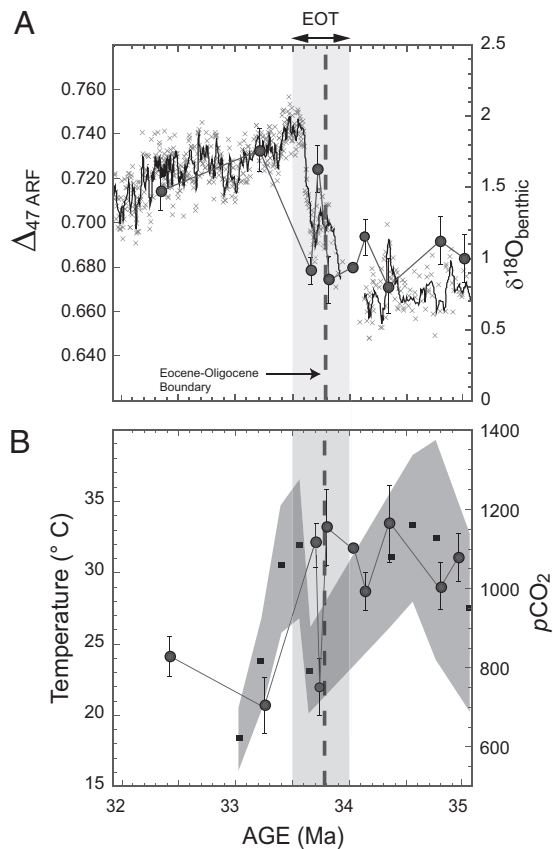
Fig. 3. (A) Δ_{47} of Hampshire Basin gastropods across the EOT. $\delta^{18}O_{benthic}$ data (gray x's) (2) are shown for reference. Error bars reflect SE of the Δ_{47} measurements. (B) Reconstructed Eocene–Oligocene atmospheric pCO_2 (squares) (5) and Δ_{47} measured temperature (circles). Error bars reflect 1 SE on multiple analyses. Vertical shaded area covers the period of the Eocene–Oligocene transition (EOT) and the dashed line indicates the Eocene–Oligocene (E-O) boundary.

During the EOT, shell $\delta^{18}O$ becomes more negative with the lowest $\delta^{18}O$ values evidenced in a shell dating to ~33.7 Ma (sample HAM S4, Fig. 2) (28). Shells from the EOT suggest a possible increase in within-shell $\delta^{18}O$ variability that may be related to an increase in seasonality or variation in water isotopes. These data are relatively limited at present; however, they show that clear variations in environmental conditions occurred during the EOT.

Δ_{47} Paleotemperatures and Paleoclimate. Relating growing season temperature to climatic conditions requires an understanding of the relationship between seasonal surface water temperature and MAAT and between bulk growth temperature and seasonal variability. The gill-breathing aquatic gastropod *Viviparus* colonizes a range of habitats and requires oxygen and fresh water. It commonly lives in deeper portions of the littoral zone during the cool season (<4 m) and migrates to shallower waters (0–2 m) during the warm growing season to avoid oxygen minimum zones. *Viviparus* can grow throughout the year but shows a decline in growth rate at cool temperatures (28). Growth rates are limited by temperature and food availability, and warm season growth rates are several times greater than cold season growth rates. In temperate lakes, *Viviparus* shows minimal growth during the cool months of September to March and rapidly grows during May and June in response to increased temperatures and food availability as photosynthetic rates increase (29). Observations of growth cessation in EOT gastropods (Fig. S3) indicate these shells dominantly record spring to summer growth (29). Collinson (16) suggested that water depths in the plant-bearing units of the Bembridge Marls Member were 0.3–3 m, so EOT snails likely record growth when located in oxygenated surface waters.

Determining the period of gastropod growth and carbonate mass accumulation in the gastropod shell is critical to relating Δ_{47} temperatures to seasonal and mean annual air temperature. The metabolic rate of freshwater fluvial and lacustrine male prosobranch gastropods is dependent upon temperature (33). In turn, shell growth rate is related to oxygen demand. Empirical measures of temperature dependence of oxygen demand for prosobranch gastropods suggest that if temperature is the primary control on shell growth, then peak carbonate mass accumulation should occur during the warm summer months, with the June to September period accounting for nearly 50% of shell growth, and the months of April to October accounting for more than 75% of total mass accumulation (*SI Methods*, Fig. S6, and Table S3). We assume that Δ_{47} temperatures of ancient *Viviparus* integrate spring to autumn water temperatures and are biased toward warm season conditions.

We used empirical lake temperature–air temperature transfer functions to interpret seasonally biased Δ_{47} temperatures with respect to MAAT (34) for a range of possible shell growing season durations. Modern surface water temperature data indicate that mean growing season water temperature is strongly correlated with seasonal and MAAT, and seasonal water temperatures can exceed air temperatures (34). Growing season water T °C ($\Delta_{47\ gastropod}$) can constrain Eocene to Oligocene MAAT (°C) when we consider water–air temperature relationships for the period of gastropod carbonate mass accumulation and growth. We consider three scenarios for shell mass accumulation to relate growing season water T °C ($\Delta_{47\ gastropod}$) to MAAT with gastropod carbonate integrating a period of growth from (*i*) April to October (*ii*), April to June, or (*iii*) June to August. Modern relationships are appropriate for an Eocene world because they include environments that are similar to the reconstructed Eocene–Oligocene climate of the Hampshire Basin.

Measured shell Δ_{47} values reflect water temperature during the growing season. Δ_{47} temperatures decrease by more than 10 °C across the EOT from peak temperatures of ~34 °C ± 3 °C to nearly 20 °C ± 2 °C (Fig. 3*B*) and closely follow patterns of deep ocean temperature change and benthic $\delta^{18}O$ (2). These show that cooling during the EOT produced a large change in water conditions during shell growth. Application of seasonally weighted transfer functions that relate seasonal temperature to MAAT enables calculation of the ΔMAAT °C during the EOT, relative to Late Eocene average MAAT (before 34 Ma). Importantly, uncertainty in the timing of growth and in which transfer function to apply does not significantly impact interpretation of MAAT as long as the period of shell growth dominantly occurs during the warm season (Table 1 and Table S1). The maximum observed ΔMAAT for a single sample level is greater than 10 °C during the EOT and Oi-1, regardless of which air–water temperature transfer function is used. If gastropod carbonate Δ_{47} is inferred to reflect April to October growth, our data indicate that MAAT decreased from a mean of ~24 °C before 34 Ma to ~18 °C in the early Oligocene (Fig. 4*A*). The assumption of a long growing season is reasonable because Eocene to Oligocene conditions were considerably warmer than present. Reconstructed temperatures closely match high-latitude paleofloral and soil tetraether paleotemperature data and are consistent with North Atlantic SST values in excess of 20 °C before the EOT (6, 7, 35). If, however, cooling during the EOT resulted in a shift in the timing of shell growth to late spring to coincide with peak food inputs, shell carbonate would be biased by water temperatures during this period. Taken together, the ΔMAAT inferred from Δ_{47} data and the shift from a longer (April to October) to a shorter growing season (April to June) would

Table 1. Measured Δ_{47} temperatures and calculated MAAT °C using water–air temperature transfer functions

| Age, Ma | Sample | n | Δ_{47} T ° C $_{ARF}$ | Calculated MAAT, °C | | | ΔT °C from pre-EOT[†,‡] |
				April–October*	April–June*	June–August*	
32.41	TBC S2	4	24 ± 2	17 ± 4	19 ± 4	13 ± 4	−7 ± 4
33.25	BOULD S5	3	20 ± 2	13 ± 4	16 ± 4	9 ± 4	−11 ± 4
33.71	BOULD S1	5	32 ± 4	25 ± 4	26 ± 5	23 ± 6	1 ± 4
33.75	HAM S13	2	22 ± 2	16 ± 4	18 ± 4	11 ± 4	−8 ± 4
33.85	HAM S5	2	33 ± 3	25 ± 4	26 ± 4	23 ± 5	1 ± 4
34.05	HAM S7	2	32 ± 3	25 ± 4	26 ± 4	22 ± 4	1 ± 4
34.16	HAM S-2	3	28 ± 4	22 ± 5	23 ± 5	18 ± 6	−2 ± 5
34.37	BEMB S3	2	34 ± 3	26 ± 4	27 ± 4	24 ± 5	2 ± 4
34.80	SCO S4	2	29 ± 4	22 ± 5	23 ± 5	19 ± 6	−2 ± 5
35.00	SCO S6	4	31 ± 2	24 ± 3	25 ± 4	22 ± 4	0 ± 4

*Weighted growth period.
[†]Calculated using mean MAAT for samples 34–35 Ma based on April to October water temperature–air temperature transfer function.
SEs reflect calibration SE for Δ_{47} temperature and calibration uncertainty plus analytical uncertainty for calculated MAAT values.
[‡]Uncertainty includes the SEM Late Eocene temperature and the uncertainty on calculated MAAT.
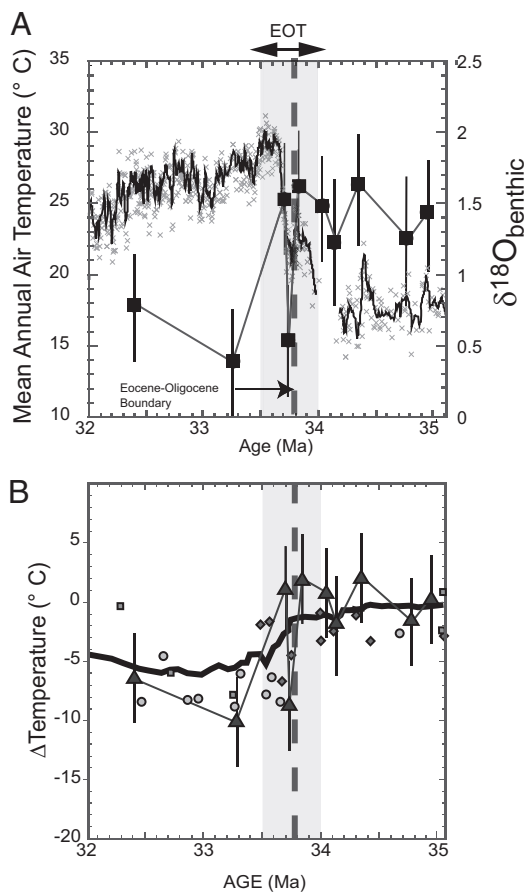
Fig. 4. (*A*) Eocene to Oligocene MAAT from Δ_{47} water temperature estimates and water–air temperature transfer function (squares). Error bars include propagated error from April to October water–air temperature transfer function calibration and SE on multiple Δ_{47} measurements. $\delta^{18}O_{benthic}$ record is shown in x's with five point running mean and reflects a combination of deep-ocean cooling and changes in ice volume (2). (*B*) Change in MAAT from Δ_{47} data (triangles) relative to Late Eocene mean (pre-34 Ma) and the ΔSST relative to Late Eocene mean for ocean drilling program sites 511 (circles), 913 (squares), and 1090 (diamonds) (7). Black line represents the smoothed change in SST °C (7). Error bars include SE of the mean Late Eocene temperature and the error associated with individual annual paleotemperature estimates.

imply a decrease in MAAT from ~24 °C before 34 Ma to ~20 °C after the Oi-1, i.e., a decrease of ~4 °C from the Late Eocene to Early Oligocene.

Hampshire Basin and Northern Hemisphere Terrestrial EOT Records. Marine records of the EOT show significant cooling during Antarctic ice buildup associated with changes in atmospheric pCO$_2$ (1, 7, 8). These show larger temperature decreases at high latitudes, whereas tropical regions show much smaller declines. Much of the cooling may occur in the lead-up to the Oi-1 onset (9) and cooling is associated with dramatically increased seasonality (9). Terrestrial records, which generally have coarser temporal resolution, show the full spectrum of climatic change during the EOT. Fossil records show a significant turnover event (Grande Coupure) coinciding with the Oi-1 or earliest Oligocene (15, 36). This turnover has been attributed to a local shift to drier conditions (36), competition from new arrivals from Asia (37), and increased seasonality (38) and lags the Eocene–Oligocene (E-O) boundary by ~100–300 ky. However, European climate records indicate significant regional climatic heterogeneity. Paleosol geochemical records from Spain show a significant decline in chemical weathering (~30%) across the EOT coincident with falling pCO$_2$, but no change

in precipitation or temperature (39). Paleosol records from the Hampshire Basin suggest minimal temperature change but an increase in precipitation across the EOT (39). Combined isotopic records of fossil teeth and carbonate from the Hampshire Basin were interpreted to show no major cooling in summer temperatures during the EOT (10). These all contrast with North Atlantic marine data that show significant cooling of the surface ocean (7).

Like European records, North American terrestrial records show a range of responses to Antarctic glaciation and declining CO$_2$. Isotopic proxies based on bone and teeth show cooling during the EOT (~8 °C) that lags global marine records by several hundred thousand years (11). North American paleosols show cooler and drier conditions across the EOT, with some sites indicating significant aridification during this transition (e.g., ref. 40). However, these records do not indicate cooling of the magnitude suggested by isotopic data from fossils (11). Paleosol and sedimentologic data would suggest that at least part of the drop in North American continental temperature during the EOT, as determined from fossil horse tooth $\delta^{18}O$, may be an artifact of changes in precipitation $\delta^{18}O$ related to changing hydrologic regimes (39).

Our clumped isotope data from the Hampshire Basin show that coastal northern Europe land temperatures decreased by an average of ~4–6 °C from the Late Eocene to the Early Oligocene. This cooling is somewhat less than the inferred cooling in continental North America (11); however, temperature declines are associated with a shift in the regional isotopic composition of ambient water. This change in water $\delta^{18}O$ may result from alteration of the regional hydrologic cycle related to global cooling and could reflect increased seasonality during and following the EOT. Importantly, Δ_{47} data from the Hampshire Basin contradict previous conventional stable isotope temperature estimates from the same localities that suggest minor or no change in growth temperatures across the EOT (10, 18). The new Δ_{47} data show a larger change in surface water $\delta^{18}O$ than was indicated by conventional fossil $\delta^{18}O$ data. Such a result suggests that reconstructed climate records based on oxygen isotopes of terrestrial carbonates are significantly improved when paired with temperature estimates that are independent of assumptions of water $\delta^{18}O$.

Δ_{47} MAAT Estimates and Atmospheric CO$_2$. pCO$_2$ decreased from >1,000 ppm to <600 ppm between 35 and 32 Ma, punctuated by a brief peak in pCO$_2$ before the marine oxygen isotope shift (5). Paleoclimate models show that a reduction of this magnitude (from 1,120 ppm to 560 ppm) should be accompanied by significant decreases in high-latitude MAAT, with much of the temperature decrease due to reductions in cold month mean temperature (CMMT) and increased seasonality (6).

Hampshire Basin Δ_{47} data show a decline in growing season temperature and MAAT (Figs. 3 and 4) during a period of declining atmospheric pCO$_2$ and the onset of major Antarctic glaciation. Pre-EOT peak CO$_2$ concentrations coincide with the highest temperatures and most isotopically enriched surface waters, which suggests that pre-EOT increases in atmospheric pCO$_2$ may have resulted in an interval of high temperatures and increased evaporation before the onset of major Antarctic glaciation. Initial phases of the EOT are characterized by an increase in local climatic variability relative to pre-EOT conditions and precede the major drop in temperature that coincides with the Oi-1 glacial event. Δ_{47} values record growing season and MAAT, but do not directly constrain seasonality.

Our data show that coastal northern Europe temperatures at ~45–50°N decreased, on average, by ~4–6 °C from the Late Eocene to Early Oligocene. This cooling was synchronous with a decrease in the concentration of pCO$_2$ and the buildup of Antarctic ice and is similar to the amount of cooling observed in North Atlantic SST (Fig. 4*B*) (7). The timescale and magnitude of terrestrial temperature decreases during the EOT indicate

coupling of terrestrial climate to atmospheric pCO_2 and ocean temperatures and suggest that rapid North Atlantic SST cooling during the EOT and Oi-1 may have resulted from a strong pCO_2–climate feedback during this critical climate transition.

Methods

Gastropod fragments were cleaned, powdered, and analyzed by X-ray diffraction. Individual shells were drilled with a micromill at a resolution of 0.4 mm for high-resolution $\delta^{18}O$. Carbonate powders were analyzed at Plymouth University, using a GV Isoprime mass spectrometer. For Δ_{47} measurements, 5–10 mg of clean powders was reacted with anhydrous phosphoric acid at 75 °C for 45 min and purified by cryogenic separation, using a glass vacuum line. Samples were reacted at 75 °C and corrected for fractionation during acid digestion on the basis of empirical measurements

(*SI Methods*). CO_2 gas was purified and transferred by passing the CO_2 gas through a 30-m Supel-Q-Plot gas chromatograph column (0.53 mm i.d.) in a He stream (flow rate of 3 mL·min^{-1}) at –20 °C and collected cryogenically for 45 min. Isotopologue measurements were determined by comparing measured values to those of a heated gas line that defines the stochastic "random" distribution. Scale compression was determined by analysis of CO_2 derived from water–CO_2 equilibration and analysis of Carrara marble samples that have been analyzed multiple times in different laboratories following established data reduction methods (*SI Methods*) (e.g., refs. 22, 41).

1. Zachos J, Pagani M, Sloan L, Thomas E, Billups K (2001) Trends, rhythms, and aberrations in global climate 65 Ma to present. *Science* 292(5517):686–693.
2. Coxall HK, Wilson PA, Pälike H, Lear CH, Backman J (2005) Rapid stepwise onset of Antarctic glaciation and deeper calcite compensation in the Pacific Ocean. *Nature* 433(7021):53–57.
3. Kennett JP, Shackleton NJ (1976) Oxygen isotopic evidence for the initiation of the psychrosphere 38 Myr ago. *Nature* 260:513–515.
4. Deconto RM, et al. (2008) Thresholds for Cenozoic bipolar glaciation. *Nature* 455(7213):652–656.
5. Pearson PN, Foster GL, Wade BS (2009) Atmospheric carbon dioxide through the Eocene-Oligocene climate transition. *Nature* 461(7267):1110–1113.
6. Eldrett JS, Greenwood DR, Harding IC, Huber M (2009) Increased seasonality in the latest Eocene to earliest Oligocene in northern high latitudes. *Nature* 459:969–973.
7. Liu Z, et al. (2009) Global cooling during the eocene-oligocene climate transition. *Science* 323(5918):1187–1190.
8. Lear CH, Bailey TR, Pearson PN, Coxall HK, Rosenthal Y (2008) Cooling and ice growth across the Eocene-Oligocene transition. *Geology* 36:251–254.
9. Wade BS, et al. (2012) Multiproxy record of abrupt sea-surface cooling across the Eocene-Oligocene transition in the Gulf of Mexico. *Geology* 40(2):159–162.
10. Grimes ST, Hooker JJ, Collinson ME, Mattey DP (2005) Summer temperatures of Late Eocene to Early Oligocene freshwaters. *Geology* 33(3):189–192.
11. Zanazzi A, Kohn MJ, MacFadden BJ, Terry DO (2007) Large temperature drop across the Eocene-Oligocene transition in central North America. *Nature* 445(7128):639–642.
12. Ivany LC, Patterson WP, Lohmann KC (2000) Cooler winters as a possible cause of mass extinctions at the Eocene/Oligocene boundary. *Nature* 407(6806):887–890.
13. Dupont-Nivet G, et al. (2007) Tibetan plateau aridification linked to global cooling at the Eocene-Oligocene transition. *Nature* 445(7128):635–638.
14. Hooker JJ, Collinson ME, Sille NP (2004) Eocene-Oligocene mammalian faunal turnover in the Hampshire Basin, UK: Calibration to the global time scale and the major cooling event. *J Geol Soc London* 161(2):161–172.
15. Hooker JJ, Grimes ST, Mattey DP, Collinson ME, Sheldon ND (2009) Refined correlation of the UK Late Eocene-Early Oligocene Solent Group and timing of its climate history. *GSA Spec Pap* 452:179–195.
16. Collinson ME (1983) Palaeofloristic assemblages and palaeoecology of the Lower Oligocene Bembridge Marls, Hamstead Ledge, Isle of Wight. *Bot J Linn Soc* 86(1–2):177–205.
17. Collinson ME, Fowler K, Boulter M (1981) Floristic changes indicate a cooling climate in the Eocene of Southern England. *Nature* 291:315–317.
18. Grimes ST, Mattey DP, Hooker JJ, Collinson ME (2003) Paleogene paleoclimate reconstruction using oxygen isotopes from land and freshwater organisms: The use of multiple paleoproxies. *Geochim Cosmochim Acta* 67:4033–4047.
19. Eiler JM, Schauble EO (2004) O-18–C-13–O-16 in Earth's atmosphere. *Geochim Cosmochim Acta* 68:4767–4777.
20. Ghosh P, et al. (2006) 13C-18O bonds in carbonate minerals: A new kind of paleothermometer. *Geochim Cosmochim Acta* 70:1439–1456.
21. Huntington KW, et al. (2009) Methods and limitations of 'clumped' CO₂ isotope (Δ_{47}) analysis by gas-source isotope ratio mass spectrometry. *J Mass Spec* 44:1318–1329.
22. Dennis KJ, Affek HP, Passey BH, Schrag DP, Eiler JM (2011) Defining an absolute reference frame for 'clumped' isotope studies of CO2. *Geochim Cosmochim Acta* 75:7117–7131.
23. White RMP, Dennis PF, Atkinson TC (1999) Experimental calibration and field investigation of the oxygen isotopic fractionation between biogenic aragonite and water. *Rapid Commun Mass Spectrom* 13(13):1242–1247.
24. Csank AZ, et al. (2011) Estimates of Arctic land surface temperatures during the early Pliocene from two novel proxies. *Earth Planet Sci Lett* 304:291–299.
25. Zaarur S, Olack G, Affek HP (2011) Paleo-environmental implication of clumped isotopes in land snail shells. *Geochim Cosmochim Acta* 75:6859–6869.
26. Huggett JM, Gale AS, Clauer N (2001) The nature and origin of non-marine 10 Å clay from the Late Eocene and Early Oligocene of the Isle of Wight (Hampshire Basin), UK. *Clay Miner* 36:447–464.
27. Huntington KW, Budd DA, Wernicke BP, Eiler JM (2011) Use of clumped-isotope thermometry to constrain the crystallization temperature of diagenetic calcite. *J Sed Res* 81:656–669.
28. Bugler MC (2011) An investigation into use of the freshwater gastropod *Viviparus* as a recorder of past climatic change. PhD dissertation (Univ of Plymouth, Plymouth, UK). Available at http://pearl.plymouth.ac.uk/handle/10026.1/531.
29. Jokinen EH, Guerette J, Kortmann RW (1982) The natural history of an Ovoviviparous snail, *Viviparus georgianus* (Lea), in a soft-water eutrophic lake. *Fresh Inv Bio* 1(4):2–17.
30. Dennis KJ, Schrag D (2010) Clumped isotope thermometry of carbonatites as an indicator of diagenetic alternation. *Geochim Cosmochim Acta* 74:4110–4122.
31. Dettman DL, Reische AK, Lohmann KC (1999) Controls on the stable isotope composition of seasonal growth bands in aragonitic fresh-water bivalves (Unionidae). *Geochim Cosmochim Acta* 63:1049–1057.
32. Sheldon ND, Costa E, Cabrera L, Garcés M (2012) Continental climatic and weathering response to the Eocene-Oligocene transition. *J Geol* 120:227–236.
33. Buckingham MJ, Freed DE (1976) Oxygen consumption in the prosobranch snail *Viviparus Contectoides* (Mollusca: Gastropoda)—II. Effects of temperature and pH. *Comp Biochem Physiol A* 53(3):249–252.
34. Hren MT, Sheldon ND (2012) Temporal variations in lake water temperature: Paleoenvironmental implications of lake carbonate δ18O and temperature records. *Earth Planet Sci Lett* 337:77–84.
35. Schouten S, et al. (2008) Onset of long-term cooling of Greenland near the Eocene-Oligocene boundary as revealed by branched tetraether lipids. *Geology* 36(2):147–150.
36. Costa E, Garcés M, Sáenz A, Cabrera L, López-Blanco M (2011) The age of the "Grande Coupure" mammal turnover: New constraints from the Eocene-Oligocene record of the Eastern Ebro Basin (NE Spain). *Paleogeog Paleoclimatol Paleoecol* 301(1–4):97–101.
37. Prothero DR (1994) The Late Eocene-Oligocene extinctions. *Annu Rev Earth Planet Sci* 22:145–165.
38. Joomun SC, Hooker JJ, Collinson ME (2010) Changes in dental wear of *Plagiolophus minor* (Mammalia: Perissodactyla) across the Eocene-Oligocene transition. *J Vertebr Paleontol* 30:563–576.
39. Sheldon ND (2009) Non-marine records of climatic change across the Eocene-Oligocene transition. *GSA Spec Pap* 452:249–259.
40. Sheldon ND, Retallack GJ (2004) Regional precipitation records from the Late Eocene and Early Oligocene of North America. *J Geol* 112:487–494.
41. Passey BH, Levin NE, Cerling TE, Brown FH, Eiler JM (2010) High-temperature environments of human evolution in East Africa based on bond ordering in paleosol carbonates. *Proc Natl Acad Sci USA* 107(25):11245–11249.

EARTH, ATMOSPHERIC, AND PLANETARY SCIENCES